Abstract. The Télescope à Action Rapide pour les Objets Transitoires (TAROT-1) has as prime objective the observation of the prompt and delayed emission of cosmic gamma-ray bursts (GRBs). We have performed a search for optical emission from 6 GRBs detected by BATSE. The positioning error circle was fully covered within typically thirty minutes after the trigger. No detection of the early afterglow phase was made, and magnitude limits in the range of $m_R = 13 - 15$ were estimated using 20s exposures. These limits are compared to optical afterglow data obtained in later phases and the results are interpreted in terms of source distances. They correspond to a median redshift of $z = 0.5$. With HETE-2 and the planned instrument upgrade, TAROT-1 will be able to detect the early optical emission of GRBs up to a redshift of the order of 5.

Key words: Gamma-Ray Bursts; Optical Afterglows

Limits on the early afterglow phase of gamma-ray burst sources from TAROT-1

M. Boër[1], **J.L. Atteia**[1], **M. Bringer**[1], **B. Gendre**[1], **A. Klotz**[1], **R. Malina**[2], **J.A. de Freitas Pacheco**[3], and **H. Pedersen**[4]

[1] Centre d'Etude Spatiale des Rayonnements (CNRS/UPS), BP 4346, 31028 Toulouse Cedex 4, France,
   email: Michel.Boer@cesr.fr
[2] Laboratoire d'Astrophysique de Marseille (CNRS/OAMP), Traverse du Siphon, BP 8, 13376 Marseille Cedex 12
[3] Observatoire de la Côte d'Azur, BP 229, 06304 Nice Cedex 4
[4] NBIfAFG, Copenhagen University Observatory, Juliane Maries Vej 30, 2100 Copenhagen Ø, Denmark

1. Introduction

Since their discovery more than thirty years ago, Gamma-Ray Bursts (GRBs) have been intriguing objects for theoreticians and challenging sources for observers. Their cosmological nature was firmly established in 1997 by observations performed by the BeppoSAX satellite (Costa, 1999), which enabled the first discovery of a faint optical transient associated to the event (van Paradijs et al. 1997). With the possible exception of GRB 980425, whose association with SN 1998bw remains in doubt (Pian et al. 1999), the measured GRB source redshifts are close to, or larger than unity. The events may be decomposed, in general, in two main phases: a prompt bursting phase, with no preferred temporal pattern, with a duration ranging from few milliseconds to several minutes (Paciesas et al. 1999); a delayed emission, the afterglow, that in a first approximation decays according to a power-law of index $\approx$ -1. BeppoSax wide-field observations were of fundamental importance for the discovery and the follow-up of the afterglow phase at different wavelengths (Costa et al. 1997, van Paradijs et al. 1997). The ROTSE experiment has given evidence for emission at optical frequencies from the prompt phase, detecting for the first time an optical burst occurring during the gamma-ray emission of GRB 990123 (Akerlof et al. 2000).

The detection of X-ray and optical afterglows of cosmic gamma-ray bursts supports the fireball model (Rees and Mészáros 1992, Mészáros and Rees 1997, Panaitescu et al. 1998) as a standard tool to interpret those observations. In this framework the afterglow emission is described as synchrotron and inverse Compton emission of high energy electrons accelerated during the shock of an ultra-relativistic shell with the external medium, while the prompt emission is due to the internal shocks produced by shells at different speeds within the relativistic blast wave

Send offprint requests to: M. Boër
Correspondence to: M. Boër

Table 1. Main technical characteristics of TAROT-1

Aperture	25 cm
Field of view	$1° \times 1°$
Optical resolution	$20\,\mu m$
Mount type	equatorial
Axis speed ($\alpha \; and \; \delta$)	adjustable, up to $80°/s$
CCD type	*Apogee AM*13 with *Kodak KAF*1300
CCD size	1080×1280 pixels
Pixel size	$15\,\mu m$
CCD readout noise	$\approx 100\,e^-$
Readout time	30 s
Filter wheel	6 pos. : Clear, V, R, I, B + V, R + I[a]

[a] Filters B+V and R+I are broad band filters covering the spectral range of respectively the Cousin B and V, and R and I filters.

(see Piran 1999 for a review). Both the prompt radiation and early afterglow phases provide us critical information to establish the physical processes during the burst itself, as well as the physical conditions of the surrounding environment (Kumar and Panaitescu, 2000, Kumar and Piran 2000). There is a general consensus that the fireball plasma is constituted by $e^- e^+$ pairs and γ-photons, however the ultimate energy reservoir and the mechanism of pair creation are still a challenge to theoretical models.

Since 1991 the Burst and Transient Experiment (BATSE, Fishman 1989) on board of the Compton Gamma-Ray Observatory (CGRO) has been detecting about one GRB source per day in the 50 - 300 keV energy band, with fluences ranging from 10^{-7}erg.cm^{-2} to 10^{-3}erg.cm^{-2}.The GRB Coordinate Network (GCN, Barthelmy 1997) uses the raw real time data of BATSE to compute very rapidly an approximate position of the sources. In spite of the large error circle of the initial coordinates, $5°$ or more, the information on the source position is transmitted in a very short time, about 4 seconds af-
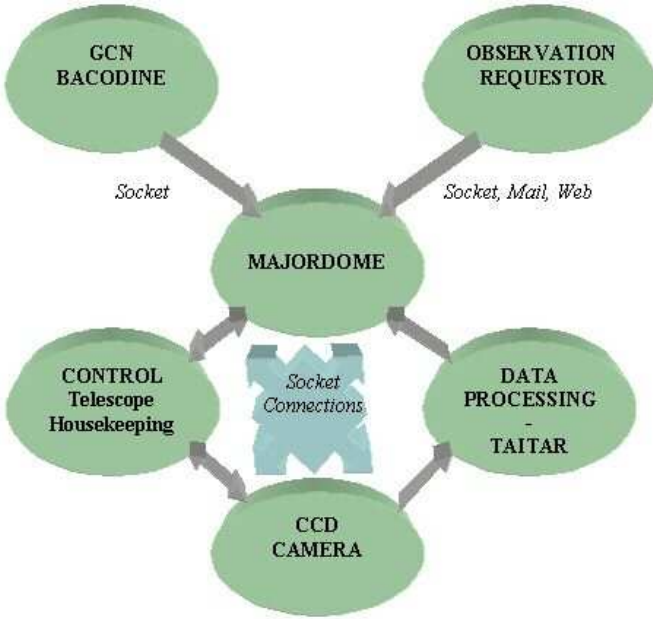
Fig. 1. The software modules of TAROT-1 and their interactions from Bringer et al. 2000. In the case of GRBs, requests are sent to the MAJORDOME by the GCN (BACODINE). The observations are immediately scheduled, and processed on line by the TAITAR software.

ter the burst triggering by the BATSE detectors. Wide field telescopes equipped with rapid optical detectors may quickly point and monitor the source position, searching for an optical transient, like the detection of GRB 990123 by the ROTSE experiment (Akerlof et al. 1999).

The aim of the *Télescope à Action Rapide pour les Objets Transitoires* (Rapid Action Telescope for Transient Objects, hereafter TAROT-1, Boër et al. 1999) is the rapid response to a triggered γ-ray event, searching for the detection of the prompt optical counterpart as well as of the early phases of the afterglow. Although this experiment was primarily designed to work in conjunction with the HETE satellite (Ricker et al. 2001), its wide field permits the observation of BATSE/GCN alerts using multiple pointings. In this paper we present the limits obtained for the early afterglow phases of sources observed during the period 1999 - 2000 detected by BATSE. These limits are interpreted in light of data obtained on GRB afterglows and in the framework of the fireball model.

2. The instrument

TAROT-1 is a fully autonomous 25 cm aperture telescope. Its 2° field of view matches well the HETE uncertainty in localization of the sources (particularly for the HETE-1 WXM, since TAROT-1 was designed before its unsuccessful launch). Table 1 summarizes the present main technical characteristics of TAROT-1.

TAROT-1 received about one observable alert from BATSE every ten days. This is in agreement with the BATSE statistics of GRB event detection, the relative night−day duration and the accessible area of the sky (10° above the North horizon to 20° for the South part of the sky). Weather conditions prevent observation during 30% of the time. Observations are performed even during the full Moon periods, although with a reduced sensitivity. TAROT-1 is fully autonomous i.e. there is practically no human intervention. Figure 1 summarizes the different software modules and their connections. All are functionally independent and the communication is made through TCP/IP socket processes.

The Telescope Control System (TCS) takes care of the instrument, performs housekeeping, weather monitoring, etc. During the night, the control is handed over by the MAJORDOME (Bringer et al. 2000), a software package in charge of the observations. In the absence of any alert from the GCN, the instrument is in *routine* mode, and observations requested by various observers are sequenced. Upon receipt of an observable GCN alert from BATSE, the ongoing observation is interrupted, and the MAJORDOME sends the telescope and camera parameters to the TCS. The reconfiguration and pointing of the telescope to its new position lasts typically 1.5 second. Taking into account the various delays involved by the GCN (4-6s), and the INTERNET socket transmission (typically 0.25s), the total reaction time, from the time of the BATSE trigger to the beginning of data acquisition, is of about of 7-10s. Since the positioning error circle of BATSE is larger than the telescope field of view, observations are performed inside a field of $25^{\square\circ}$, covered by a set of 5×5 mosaic. In the best cases this total field covers only the 68% confidence radius of the error circle, including statistical errors, as discussed in the BATSE 4B catalog (Paciesas et al. 1999). TAROT-1 reacts to BATSE_LOCBURST notices (see the GCN web site: http://gcn.gsfc.nasa.gov for a description of the various notice types). After usually 20s to 10min, a new alert is sent by the GCN, called BATSE_FINAL, with improved coordinates, producing a second positioning of TAROT-1, and the start of a new mosaic. If the difference between the BATSE_LOCBURST and BATSE_FINAL positions is less than 1° the telescope keeps its current position. Depending on the burst brightness, the Huntsville BATSE team may compute a better position, which is usually transmitted by the GCN 30 to 60min later. TAROT-1 moves accordingly and eventually reduces the area explored, depending on the actual uncertainty. During the remaining of the night, a continuous coverage of the area is maintained, trying to detect and to keep track of an eventual optical transient.

As soon as an image is obtained, the image processing software (called TAITAR in figure 1) produces a source catalog. Presently, the generated list of sources is compared to the USNO catalog both for astrometric and photometric reductions. Once TAROT-1 has completed a full

Table 2. TAROT-1 observation log for the GRB source observations made with CGRO-BATSE

Source name	BATSE trigger time (UT)	Error circle radius(°)[a]	Matching with mosaic? (see text)	Sky conditions	Moon phase (%)
GRB 990802	01 : 04 : 44	2.1	Full	Clear	70
GRB 990807	21 : 55 : 46	2.5	No match	Clear	No Moon
GRB 990903	19 : 14 : 56	2.7	Partial	Partly cloudy	No Moon
GRB 990915	23 : 15 : 23	2.2	Full	Clear	No Moon
GRB 990917	20 : 12 : 28	2.6	Partial	Clear	50
GRB 991002	22 : 49 : 03	2.8	Full	Clear	45
GRB 991115	18 : 48 : 08	2.2	Partial	Cloudy	45
GRB 991129	22 : 38 : 08	4.0	No match	Clear	50
GRB 991211	04 : 34 : 42	6.1	No match	Clear	No Moon
GRB 000107	00 : 44 : 09	6.8	No match	Clear	No Moon
GRB 000111	02 : 41 : 58	5.2	Partial	Clear	No Moon
GRB 000201	03 : 02 : 09	2.1	Full	Clear	25
GRB 000221	23 : 39 : 10	2.0	No match	Partly cloudy	85
GRB 000225	01 : 35 : 29	2.3	Full	Partly cloudy	62
GRB 000226	03 : 51 : 49	2.5	Partial	Clear	55
GRB 000229	02 : 45 : 02	2.4	Full	Cirrus clouds?	35
GRB 000302	02 : 50 : 25	2.1	No match	Clear	No Moon
GRB 000312	20 : 50 : 50	2.5	Full	Clear	45
GRB 000321	21 : 53 : 08	4.1	Partial	Partly cloudy	90
GRB 000408	02 : 35 : 48	2.5	Partial	Clear	No Moon
GRB 000418	21 : 30 : 17	5.4	No match	Clear	100

[a] 68% confidence radius from the last available BATSE data, taking into account both statistical and systematic errors.

mosaic, an e-mail message is sent, and a scientist on duty is paged to compare the images and to look for possible new sources. The images are acquired without filter (clear position in the filter wheel) and with an exposure time of 20s. With the APOGEE camera the readout time was 30s, hence the total time needed to observe the full mosaic was 21 min.

3. Observations and reduction

TAROT-1 observations of GRBs started routinely in 1999, although the data for the first half of July 1999 has been lost because of a hardware failure of the media recorder . All observations are summarized in table 2. The two first columns give the GRB date and time. The third column give the error circle taken from the final data reduction provided by the BATSE team, including the systematic error as given in Paciesas et al. (1999). For several sources, it appears that neither the BATSE_FINAL nor the BATSE_LOCBURST positions were accurate enough to match fully our mosaic. This indication is given in column 4, while the sky conditions are depicted in the next column, with the Moon phase in the 6th column. The influence of the Moon depends on its phase and distance to the source, and has an impact on the upper limits we computed. A phase of 30% begin to produce a higher background whatever the Moon position over the sky. No event observed by TAROT-1 as a response to a BATSE/GCN

alert was detected by another instrument, whatever the wavelength. In six cases, the 68% error circle has been adequately sampled and the sky conditions were correct, hence the probability that TAROT-1 never observed a burst source (i.e. the six sources are outside their 68% error circle) is 0.0011, assuming a uniform probability distribution over the error circle. Of course, the detection probability depends on the unknown source magnitude. Hence the source detection probability will be $(1-0.68p)^6$, where p represents the fraction of bursts above the TAROT-1 detection threshold at the time of observation.

Since no optical sources were detected, a 3σ upper limit to the magnitude was calculated by comparing several stars on the images with the USNO A2.0 catalog. Since observations were performed without any filter, a correction factor was estimated in order to provide a R-magnitude upper limit, assuming an energy spectral index equal to 1. Under this condition, one finds that the correction to be applied to the measured TAROT magnitude m_T is $R = m_T - 0.4$. The limits obtained are listed on table 3 as a function of the elapsed time since the BATSE trigger. The delays mentioned in the second column corresponds to the end of the scan matching the final BATSE source position.

Table 3. 3σ upper limits (transformed in R magnitude) to the GRB source counterparts for the 6 well observed events mentioned in table 2.

Source name	Time since trigger (days)	3σ upper limit (R magnitude)
GRB 990802	0.0200	12.7
	0.0402	13.2
GRB 990915	0.0404	13.9
	0.0719	14.1
GRB 991002	0.0231	13.0
	0.0441	12.9
	0.0643	14.3
	0.0971	14.2
	0.1299	12.8
GRB 000201	0.0177	13.3
	0.0317	15.3
	0.0504	15.3
	0.0723	15.1
	0.0885	14.9
GRB 000229	0.0192	14.2
	0.0942	14.3
	0.1321	15.2
GRB 000312	0.1033	14.7

4. Discussion

TAROT-1 upper limits on the optical flux of GBR 990123, the only source until now detected both during its prompt and afterglow phase, were compared with ROTSE data. Figure 2 displays TAROT-1 upper limits and ROTSE measurements (Akerlof et al. 1999), as well as later data (Galama et al. 1999).

Another possibility is to compare TAROT-1 upper limits with data obtained for GRB afterglows at later times. The result of this comparison is displayed in figure 3, whereas the basic data and references are given in table 4. We note that in the time region observed by TAROT-1, GRB 970508, GRB 980519, GRB 991208, and GRB 991216, in addition to GRB 990123,would have been detected by TAROT, if we extrapolate the late epoch afterglow to early times. Of course, this is a crude extrapolation which does not take into account possible breaks in the light curves.

We tried to evaluate the possible effect of the source distance on the burst afterglow detection by TAROT-1. To perform this task we have to correct for the galactic absorption and for the source distance (Boër and Gendre 2000). We have scaled the flux of sources with known distances to a common redshift of $z = 1$, applying corrections for distance, time dilation and absorption in our galaxy (Schlegel et al. 1998). We assume a flat cosmology with $\Omega_\Lambda = 0.7$ and $H_0 = 65$km.s^{-1}.Mpc^{-1}. Table 5 gives the corrections computed and the decay indexes. The corrected light curves are displayed in figure 4 together with TAROT-1 upper limits. As it can be seen, extrapolating to
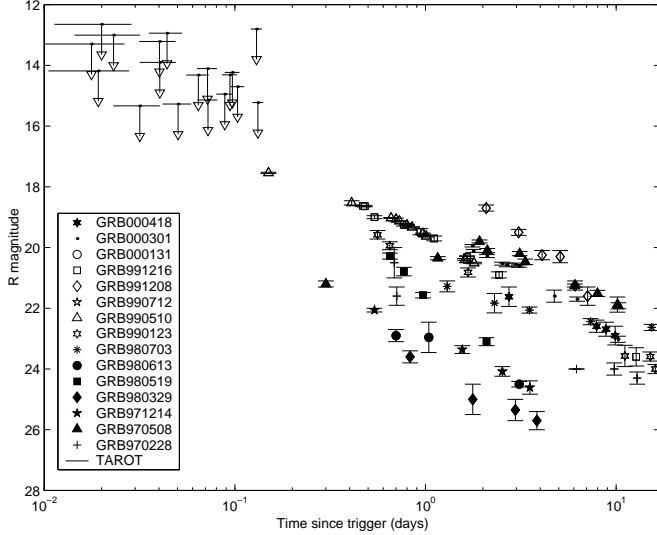
Table 4. The GRB source sample used for comparison of the known afterglow light curves with our upper limits. Column 3 indicates the decay index after correction from

Source	Redshift	References
GRB 970228	0.695	1, 2, 3, 4
GRB 970508	0.835	5 − 10
GRB 971214	3.42	11
GRB 980329	–	12
GRB 980519	–	13 − 15
GRB 980613	1.096	16 − 18
GRB 980703	0.966	19
GRB 990123	1.61	20, 21
GRB 990510	1.62	22, 23
GRB 991208	–	24 − 26
GRB 991216	1.02	27 − 33
GRB 000301c	–	34 − 40
GRB 000418	1.12	41 − 43

1 Guarnieri et al., 1997
2 Metzger et al. 1997
3 Pedichini et al. 1997
4 van Paradijs et al. 1997
5 Fruchter et al. 1997
6 Galama et al. 1997
7 Garcia et al. 1997
8 Djorgovsky et al. 1997
9 Mignoli et al. 1997
10 Pedersen et al. 1998
11 Diercks et al. 1998
12 Reichart et al. 1999
13 Bloom et al. 1998a
14 Gal et al. 1998
15 Vrba et al. 2000
16 Djorgovsky et al. 1998
17 Halpern et al. 1998
18 Hjorth et al. 1998
19 Bloom et al. 1998b
20 Akerlof et al. 1999
21 Galama et al. 1999
22 Harrison et al. 1999
23 Staneck et al. 1999
24 Kuulkers et al. 2000
24 Castro-Tirado et al. 1999
25 Jensen et al. 1999a
26 Masetti et al. 1999
27 Djorgovsky et al. 1999
28 Dolan et al. 1999
29 Garnavich et al. 1999
30 Henden et al. 1999
31 Jensen et al. 1999b
32 Jha et al. 1999
33 Sagar et al. 2000
34 Bernabei et al. 2000
35 Fynbo et al. 2000
36 Gal-Yam et al. 2000
37 Garnavich et al. 2000
38 Halpern et al. 2000
39 Mohan et al. 2000
40 Veillet and Boër 2000
41 Henden 2000
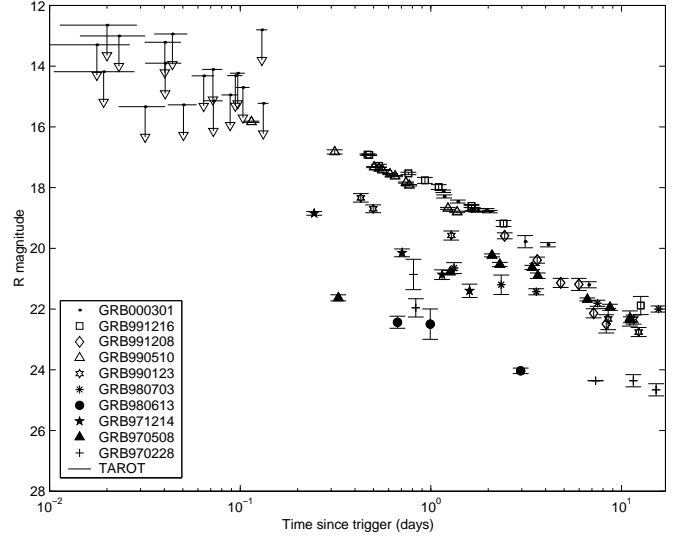42 Henden and Klose 2000
43 Mirabal et al. 2000
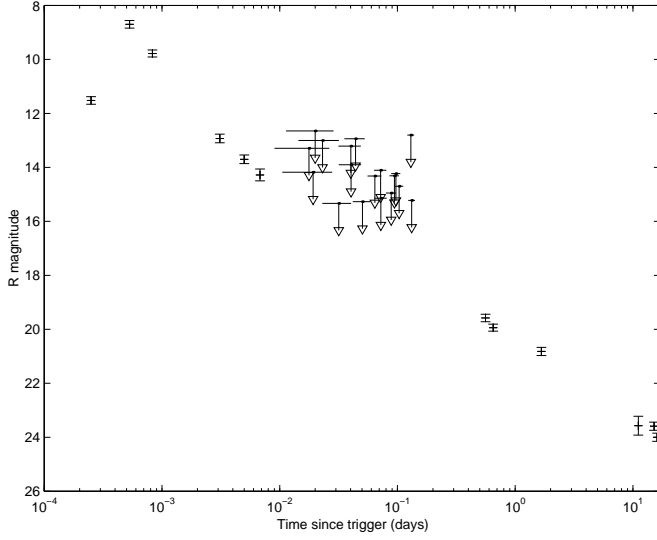
Fig. 2. Comparison between the TAROT upper limits (arrows) and the light curve of GRB 990123 (error bars). Both the prompt and the afterglow emission are shown. Data from Akerlof et al. (1999) and from Galama et al. (1999)

Fig. 3. Comparison between the TAROT upper limits (arrows, all data) and the afterglow light curve of GRB sources detected at optical wavelengths (table 4). In this figure, the light curves have not been corrected

Fig. 4. Comparison between the TAROT upper limits (arrows, all data) and the afterglow light curve of GRB sources. The light curves have been normalized to a common distance corresponding to a redshift of 1, according to the method described in the text (Boër and Gendre 2000) and using the data from table 5. We took into account the K-correction, distance and time dilation, and absorption from our Galaxy (table 5).

5. Conclusions and perspectives

In this paper, the lower R-magnitude limit for the early afterglow light curves of GRB is computed, for sources observed by TAROT-1 after its first year of routine operation. These limits are compared with the optical afterglow data obtained so far. A maximum source distance of z = 1.2 was estimated for observations made with TAROT-1 one hour after the GRB main event begins. The accuracy of HETE-2 (Ricker et al., 2001) or SWIFT (Gehrels, 2000) will allow to start the observation within few seconds after the GRB triggers the detectors, while for BATSE we had to scan the error circle, an operation lasting 30 minutes. Given the expected HETE-2 detection rate of 40 events per year in the anti-solar direction, TAROT-1 may expect to observe a source location once every month. In order to estimate the maximum source distance TAROT-1 can reach, we extrapolate the light curves plotted on figure 4 to a time of five minutes after the burst onset. In this case, the median redshift corresponding to a limiting magnitude of 15 is z = 1.2.

In addition, the detector will soon be replaced by a camera based on a Thomson 7899 CCD. It will have a total noise of 10e⁻, for a readout time of 1 second, allowing to reach the 17th R magnitude in 10 seconds. With this new device TAROT-1 will be able to monitor the GRB optical light curves, not only during the prompt event, but also the transition between the prompt and afterglow phase. After five minutes, even in the worst case discussed

the proper time domain, TAROT-1 would have detected 5 events, if their redshift would have been equal to z = 1.

These data can also be used to estimate the limiting TAROT-1 distance of detection. Assuming a limiting magnitude of 15 one hour after the burst, the corresponding distance is z = 1.2 for the brightest burst and 0.1 for the faintest one, the median redshift being 0.5.

Table 5. Distance and galactic absorption correction factors for the GRB sources of known distance. These quantities are used to normalize the GRB light curves to a common distance corresponding to a redshift of 1 (see text). The corrected power law decay index is tabulated column 5 (for details see Boër and Gendre, 2000)

| Source | *Correction factors* | | | |
	Correction for distance	*K−Correction*	*Galactic absorption*	*Corrected light curve decay index*
GRB 970228	0.41	1.0	0.61	1.10 ± 0.11
GRB 970508	0.64	1.0	0.05	1.17 ± 0.21
GRB 971214	20.2	1.2	0.06	1.20 ± 0.27
GRB 980613	1.10	1.0	0.22	1.00 ± 0.01
GRB 980703	0.92	1.0	0.72	1.17 ± 0.25
GRB 990123	3.23	0.9	0.04	1.44 ± 0.07
GRB 990510	3.28	0.9	0.53	1.54 ± 0.15
GRB 991216	1.05	1.0	1.67	1.22 ± 0.04

in section 4 (z = 0.1, one hour after the burst onset with the previous camera) the TAROT-1 distance limit will correspond to a redshift of 2, and the median redshift of 5.6, while after 1 hour, this distance will still correspond to a median redshift of 2.2 (0.5 with the previous camera).

Already in its current configuration TAROT-1 is able to give stringent limits to the early afterglow phase. In conjunction with a satellite like HETE-2 or SWIFT, the transition between the prompt and delayed mode will be monitored, allowing to acquire critical data on GRB sources.

References

Akerlof, C., et al., 1999, Nat 398, 400

Akerlof, C., et al., 2000, ApJ 532, L25

Barthelmy, S., 1997, Proceedings of the 4th Huntsville Symposium, AIP conf. proc. 428, edts. C.A. Meegan, R.D. Preece, and T.M. Koshut, p. 99.

Bernabei, S., et al., 2000, GCNC 599

Bloom, J.S., et al., 1998a, GCNC 87

Bloom, J.S., et al., 1998b, ApJ 508, L21

Boër, M., et al., 1999, A&AS 138, 579

Boër, M., and Gendre, B., 2000, A&A 361, L28

Bringer, M., Boër, M., Peignot, C., Fontan, G., Merce, C., 2000, Exper. Astrophys. *submitted*

Castro-Tirado, A.J., et al., IAUC 7332

Costa, E., et al. 1997, Nat. 387, 783

Costa, E., 1999, A&AS 138, 425

Diercks, A., et al., 1998, ApJ 503, L105

Djogovski, S.G., et al., 1998, IAUC 6660

Djogovski, S.G., et al., 1998, GCNC 117

Djogovski, S.G., et al., 1999, GCNC 510

Dolan, C., et al., 1999, GCNC 486

Fishman, G., et al., 1989, Proc. Gamma-Ray Observatory science workshop, W.N. Johnson edt., GSFC Greenbelt, p. 2

Fruchter, A., et al., 1997, IAUC 6674

Fynbo, J.P.U., et al., 2000, GCNC 576

Gal, R.R., et al., 1998, GCNC 88

Galama, T. et al., 1997, IAUC 6655

Galama, T. et al., 1999, Nat 398, 394

Gal-Yam, A., et al., 2000, GCNC 593

Garcia, L., et al., 1997, IAUC 6661

Garnavich, P., et al., 1999, GCNC 495

Garnavich, P., et al., 2000, GCNC 581

Gehrels, N., 2000, Proceedings of the 5th Huntsville Symposium, AIP conf. proc. 526, edts. R.M. Kippen, S. Mallozzi, and G. Fishman, p. 671.

Guarnieri, A., et al., 1997, A&A 328, 13

Halpern, J.P., et al., 1998, GCNC 134

Halpern, J.P., et al., 2000, ApJ, *in press*

Harrison, F.A., et al., 1999, ApJ 523, L121

Henden, A., et al., 1999, GCNC 473

Henden, A., 2000, GCNC 652

Henden, A., and Klose, S., 2000, GCNC 656

Hjorth, J., et al., 1998, GCNC 109

Jensen, B.L., et al., 1999, GCNC 454

Jensen, B.L., et al., 1999, GCNC 498

Jha, S., et al., 1999, GCNC 476

Kumar, P., and Panaitescu, A., 2000, astro-ph 0006317

Kumar, P., and Piran, T., 2000, ApJ 535, 152

Kuulkers, E., et al., P., 2000, ApJ 538, 638

Masetti, N., et al., 1999, GCNC 462

Mészáros, P., and Rees, M., 1997, ApJ 476, 232

Metzger, M., 1997, IAUC 6588

Mignoli, M., 1997, IAUC 6661

Mirabal, N., 2000, GCNC 653

Mohan, V., et al., 2000, GCNC 595

Paciesas, W.S., et al., 1999, ApJS 122, 465

Panaitescu, A., Mészáros, P., and Rees, M., 1998, ApJ 503, 314

Pedersen, H. et al., 1998, ApJ 503, 314

Pedichini, F., et al., 1997, A&A 327, 36

Pian, E., et al., 1999, A&AS, 138, 463

Piran, T., 1999, Phys. Rep. 314, 575

Rees, M., and Mészáros, P., 1992, MNRAS 258, 41

Reichart, D.E., et al., 1999, ApJ 517, 692

Ricker, G.R., et al., 2001, A&AS *in press*

Sagar, R., et al., 1999, Bull. Astron. Soc. India 28, 15

Schlegel, D.J., Finkbeiner, D.P., and Davis, M., 1998, ApJ 500,
    525

Stanek, K.Z., et al., 1999, ApJ 522, L39

van Paradijs, J., et al., 1997, Nat 386, 686

Veillet, C., and Boër, M., 2000, GCNC 598

Vrba, F., et al., 2000, ApJ 528, 254